Journal of the Physical Society of Japan
Vol. 71, No. 4, April, 2002, pp. 1189–1196

Free Surface Flow and Fracture in Granular Media

Abraham MEDINA

Grupo de Medios Porosos y Granulados,
Programa de Yacimientos Naturalmente Fracturados, IMP. 07730 Mexico, D.F., Mexico

(Received October 26, 2001)

Granular media, like sand and powders, are very complex in their dynamics. Due to it there is not yet a set of equations valid over a wide range of several motion regimes. In this work we present a simple and unified analytical approach which takes into account the Coulomb's yield criterion (CYC) for the description of the free surface deformation in non cohesive granular media and the rupture patterns in cohesive granular media. Through the discussion of some examples and its comparison with experiments we show the usefulness and necessity of this criterion in this kind of problems.

KEYWORDS: mechanics of discrete systems, granular matter, free surface flow
DOI: 10.1143/JPSJ.71.1189

1. Introduction

Recently, granular matter has received special attention from the research community (see, for instance, the reviews in refs. 1–5). The diverse set of behaviors of granular materials in nature and in industry have made difficult its description. So, several of the main factors which make the study of granular material an interesting subject of research, are among others: i) The lack of general equations of motion and constitutive relations valid over a wide range of flow regimes, and ii) the existence of unique phenomena that characterize these materials, such as segregation (the spatial separation of the material in zones of different grain sizes) (see, for instance, refs. 6 and 7), dilatance (increase in the occupied volume by the granular medium by compression),[8,9] arching (which causes independence of the hydrostatic pressure on the height in vessels enough filled with granular material),[5,10] etc.

Other phenomenon not very well understood which appears very commonly in these materials is surface fluidization.[11–14] Qualitatively, in a heap of non cohesive granular material, the most simple case of fluidization can be developed on its free surface under the gravity action. The start of this continuous distortion of the surface (yield) is approximately governed by the Coulomb's yield criterion (CYC)[15–19] and occurs when the slope of the heap reaches a maximum value (the angle of internal friction ϕ_c) at which the pile's surface yields, producing a granular flow or avalanche. In relation with this flow a general behavior appears: When the angle of internal friction is reached, slowly, the resulting flow is slow and slightly dissipative. However, a more rapid and strongly dissipative flow can be produced when this angle is reached rapidly; both facts will be very much exploited later. In this yield limit, named the plastic limit, the free surface and the overall material can be changed. The CYC also may be reached in systems under external forces and the motion equation for these systems gives interesting results. Similarly, the fracture phenomenon in cohesive granular materials can be described by the CYC. We will show that such a phenomenon can be useful, for instance, in order to evaluate material properties such as the cohesion level of a given sample.

Our goal in this work is to study the granular gravity flow on a free surface and the rupture process from a macroscopic or continuum point of view. This approach has strong limitations in the study of granular media,[4,5] but in the (steady) problems here treated it has been very useful and precise. A direct comparison with experimental results, if these exist, will be made in order to show also the limitations of this approach. So, this paper is structured as follows. In §2 we describe and model the main granular flow regimes, the balance of forces equation for the steady-state, fully dynamic regime is derived through a micromechanical approach for the dissipative stress term and directly the balance of forces equation is obtained for the quasi-static regime. In §3 we present some analytical solutions of the balance equations for the surface granular flow induced by gravity and other external forces; we treat the rapid granular flow on the free surface originated during the rotation of a cylinder about its horizontal axis. In case of quasi-static regime we present the problems, respectively, of the surface's shape in a rotating thin rectangular bin and of the free surface deformation under an rectilinear uniform acceleration. In §4 we treat the convenience and usefulness of an universal description for the fracture patterns in cohesive granular media under axisymmetrical rotation of a sample of cylindrical shape.[20] Comparison with experimental data (obtained for a xerographic developer)[21] let us collapse, when appropriately normalized, into one universal curve both limits of high and low cohesion. This fact clearly simplifies the physical description of this phenomenon. Finally, in §5 we discuss the advantages and limitations of the continuum models based on the CYC and we present the conclusions of this work.

2. Fully Dynamic and Quasi-Static Granular Flow

From a continuum point of view, there are at least two regimes for the granular flow:[11,12] a) a rapid flow regime, called by Bagnold the *fully dynamic* or *fluidlike grain-inertia* regime, where high shear rates dominate, the interstitial fluid plays a minor role, and moderate packing factors or concentrations are of importance, and b) a slow flow regime, called also by Bagnold the *quasi-static* or rate-independent plastic regime, with vanishing shear rates and high packing factors.

Our starting point in discussing the rapid granular flow regime, is the formulation of a micromechanical steady-state model to justify the quadratic form of the dissipative term in the stress balance equation. Such model is based on the

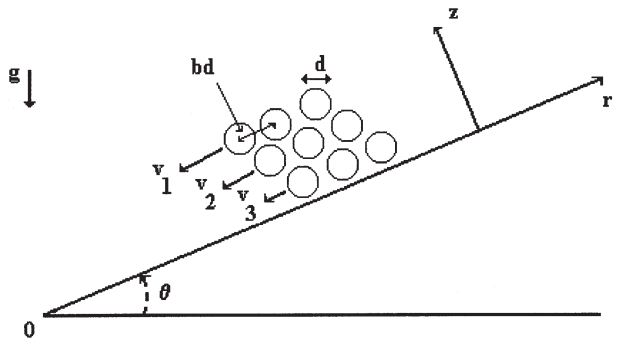

Fig. 1. Simplified model of the grains motion during the rapid granular flow, at the angle θ. The separation between grains along the r axis is $s = bd - d$, where d is the grain diameter.

assumption that the material is constituted by rigid, monodisperse grains which form adjacent thick frictional *layers* (see Fig. 1). Each layer, at an angle θ respect to the horizontal ($\theta > \phi_c$), contain grains whose size and nearest-neighbor distance are roughly comparable, but coordinates and velocities are assumed to be continuous. The gradient of the velocity v is supposed to be in the z-direction perpendicular to these layers, so that on the average the upper layer moves respect to the lower layer with relative velocity Δv. This not meant to imply that the motion necessarily occurs in these ordered assemblies, but is intended to focus attention on the difference in the mean velocities of the neighboring grains.

The more realistic aspects of the grain motion, like packing (different grain concentrations), collision conditions and grain rotation will be included through a proportionality factor whose form can be justified by using dimensional analysis. From the derived equation of motion, the force balance equation for the slow flow regime can be obtained just by making the shear rate tend to zero.

For the fully dynamic regime, an elementary approach based on Coulomb's balance of stress available for statics, to which will be add a dissipation term due to interparticle collisions has been recently proposed. So, the mechanism for the dissipative stress generation incorporate the non-Brownian particle motion during the rapid non-cohesive flow which has a momentum loss at each collision and a collision rate proportional to ∇v, where v is the average grain velocity, then the shear stress varies as $\tau \sim (\nabla v)^2$. It can be understand, in accordance with Bagnold as follows: When grain collisions occur between two adjacent layers, an average net momentum proportional to Δv in the $-r$-direction (direction of flow) is transferred. Since the collision rate (the inverse of the collision time $\Delta z/\Delta v \sim \partial z/\partial v$) is proportional to $\partial v/\partial z$, the shear stress τ exerted by the upper layer, on the lower layer, in the $-r$-direction, is $\tau \sim \Delta v(\partial v/\partial z)/(\Delta z)^2$. Considering, as aforementioned, more realistic aspects of the grain motion, the shear stress can be put in the form

$$\tau = \alpha\left(\nabla v\right)^2, \tag{1}$$

with $\alpha = a\cos\eta\rho_p\lambda d^2 h(\lambda)$, where λ^{-1} is called the dilatance and its inverse, $\lambda = d/s$, is the linear concentration. In accordance with Fig. 1, d is the grain diameter, s is the mean separation between grains along the flow direction $-r$, $s = bd - d$, ρ_p is the grain density, $h(\lambda)$ is an unknown function which takes in to account the concentration, η corresponds to the angle whose tangent is the ratio of the tangential to the normal component of the stresses, and a is a constant. If the spheres are not perfectly matched or if the shearing were to take place along parallel curved surfaces, we might expect general shearing to be possible at some value of λ. For lower values of λ the grains should pass one another with progressively greater freedom.

The principal result of Bagnold's model, outlined above, can be derived from a more simple reasoning. We propose a steady-state model in which the dissipative force originates from the interaction between single grains, due to their relative velocity. When the static friction force has been overcome, the system begins to flow. Due to high shear rates, each grain is mainly affected by the adjacent grain layers through a force which is quadratic in the mean relative velocity.

This approximation can be justified by considering the motion of a single grain with relative velocity v_r on a grain layer at the angle $\theta \gtrsim \phi_c$. In steady granular flow, the relative mean velocity is constant. This can occur when the change in potential energy, along an elementary path $\delta r = d$ (defined as the distance between two successive collisions or between neighboring beads), is just the energy lost in inelastic collisions and by friction, given as

$$\left\langle E_p \right\rangle \approx dm_p g\sin\theta = \frac{\varepsilon}{2} m_p v_r^2 + d\mu m_p g\cos\theta. \tag{2}$$

Here m_p is the grain mass, ε is the collision coefficient, g is the gravity acceleration and $\mu = \tan\phi_c$ corresponds to the material parameter called the coefficient of friction. In the last term of this equation we have used the CYC[15] which states for a non cohesive granular medium that the frictional forces f and the normal forces N are related by the form $|f| \le N\mu = N\tan\phi_c$. When the equality is reached, the grain starts the motion and a flow occurs. By dividing eq. (2) by d, we obtain the force balance equation in the $-r$-direction on a single grain as

$$-\frac{\varepsilon}{2d} v_r^2 + g(\sin\theta - \mu\cos\theta) = 0. \tag{3}$$

This model predicts very well the observed mean velocity in experiments.[22]

In order to obtain the equation of motion for the granular flow on the free surface on the basis of the above model, we should consider the existence of several adjacent grain layers. In accordance with Fig. 1, the grains in the upper layer have an average velocity v_1, the grains in the intermediate layer have an average velocity v_2 and, those in the third layer have an average velocity v_3. Experimental evidence also shows that the average velocity of grains in the deep layers along the downward normal tend rapidly to zero.

Under the action of gravity, two frictional forces act on each grain; One is static (according to the CYC, proportional to the normal force), while the other is of a dynamic nature. We now pay attention to the dynamic process, where grain motion is such that the frictional forces between the particle which have an average velocity v_2 and the others gives a resultant force which can expressed in terms of Taylor's series around $z = z_2$, where z is the normal coordinate and z_2 is the corresponding of the grain with velocity v_2. $z_2 + d$ is

the coordinate of the grain with velocity v_1 and $z_2 - d$ is the coordinate of the grain with velocity v_3. Assuming a continuous variation of the average velocity in the coordinates, expanding and redefining $v_2 = v_r$, we find that $v_{2\pm1} = v_r \pm (\partial v_r/\partial z)_{z_2} d$. This series can be truncated only for small values of the ratio of the particle size to the thickness of the granular flow, $d/D \ll 1$.

The resultant force acting on the intermediate grain can be then given by

$$F = k\left((v_3 - v_2)^2 - (v_2 - v_1)^2\right) \approx 2k\gamma\gamma' d^3 = kd^3 \frac{\partial}{\partial z}\left(\frac{\partial v_r}{\partial z}\right)^2, \tag{4}$$

where k is a factor taking into account the collisions nature, as later on will be shown, $\gamma = (\partial v_r/\partial z)$ is the shear rate and $\gamma' = (\partial^2 v_r/\partial z^2)$. The shear stress is then given by

$$\tau = k\left(\frac{\partial v_r}{\partial z}\right)^2. \tag{5}$$

Close to the surface at the angle θ, where fluidization has begun, the *one grain* analysis can be extended to an intermediate material element of bulk density ρ. In this last case, comparing the eq. (5) with eq. (1) we found that $k = \alpha$ and, therefore, the stress balance equation that includes both the static stresses through the CYC and the dissipative dynamic friction, is

$$\alpha\left(\frac{\partial v_r}{\partial z}\right)^2 - \rho g z(\sin\theta - \mu\cos\theta) = 0, \tag{6}$$

The corresponding force balance equation is then

$$\alpha\frac{\partial}{\partial z}\left(\frac{\partial v_r}{\partial z}\right)^2 - \rho g(\sin\theta - \mu\cos\theta) = 0, \tag{7}$$

which is the generalized form of eq. (3) and agrees, for example, with the model used to describe the rapid granular flow inside rotating horizontal cylinders.[23] Like other continuum theories another way to find the form of α is through experiments. To our knowledge this has not been made.

In the quasi-static regime, i.e., when slow flow is occurring, the shear rate vanishes and high packing factors are dominant.[10–13] This case corresponds to the plastic behavior of a frictional Coulomb material of the kind that has been studied extensively in the context of soil mechanics.[16,17] Particles can stick together, roll, or maintain sliding contact with one another for extended periods and deformation inertial forces in the bulk are transmitted from one region to another through a network of contact forces. During the initial flow, granular materials can experience an increase or decrease in the volume depending on the initial state of the material;[10,16] however with continuous deformation, the material tends towards an asymptotic state with constant volume.

Finally, the force balance equation for slow flow regime can be obtained just by making the shear rate tend to zero in eq. (7), it yields

$$\rho g(\sin\theta - \mu\cos\theta) = F_B, \tag{8}$$

where F_B is the steady state body force, per unit volume, acting on the granular surface. This last force has two terms: the driving and its corresponding friction forces.

3. Some Analytical Solutions for Surface Flow

We present some analytical solutions for eqs. (7) and (8), by studying the rapid flow regime (continuous flow) in a horizontal rotating cylinder and the slow flow regime during the vertical rotation of a bin and during the uniform acceleration of a box of sand. All the solutions to these problems give closed form expressions, which are in good agreement with experimental observations.

3.1 Flow in a cylinder with horizontal rotation

The rotation of a cylinder about its horizontal axis, half filled with sand, has been studied due its related phenomena of discrete and continuous flow regimes.[23] The discrete regime occurs for low angular velocities while the continuous regime, Fig. 2, occur when the angular velocity Ω is larger than two critical values Ω_1 or Ω_2, depending on if these values of the angular velocity were reached coming up or going down. In particular, in the continuous flow regime, a rapid granular flow takes place on the surface which can be characterized experimentally by the current, J which seems to obey the law

$$J \sim (\theta - \phi_c)^m, \tag{9}$$

where $m = 0.5 \pm 0.1$ and $\theta > \phi_c$. eq. (9) implies a direct relation between the surface current and the slope, not depending on the detailed geometry of the container. However, a more detailed expression can be obtained through a continuum model using directly the eq. (7). In fact, taking the z axis normal to the flow and oriented, unlike Fig. 1, downward, we found a solution of the eq. (7) in terms of a limited expansion, near $\theta = \phi_c$ of the form

$$v(z) = \frac{2}{3}\left(\frac{\rho g h^3}{\alpha}\cos\phi_c\right)^{\frac{1}{2}}\left[1 - \left(\frac{z}{h}\right)^{\frac{3}{2}}\right](\theta - \phi_c)^{\frac{1}{2}}, \tag{10}$$

where h is the thickness of the granular flow. The current J is given by

$$J = \frac{2}{5}\left(\frac{\rho g h^5}{\alpha}\cos\phi_c\right)^{\frac{1}{2}}(\theta - \phi_c)^{\frac{1}{2}}, \tag{11}$$

which agrees with the experimental power law (9) and also, does not depend on the geometry.

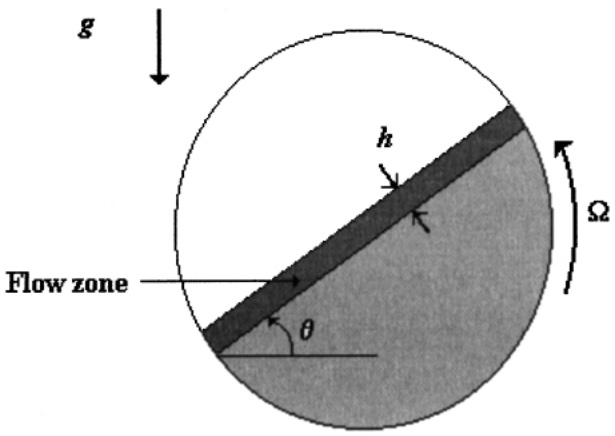

Fig. 2. Schematic view of the half-filled horizontal rotating cylinder. Ω is the angular velocity, g is the gravity acceleration and R is the cylinder's radius.

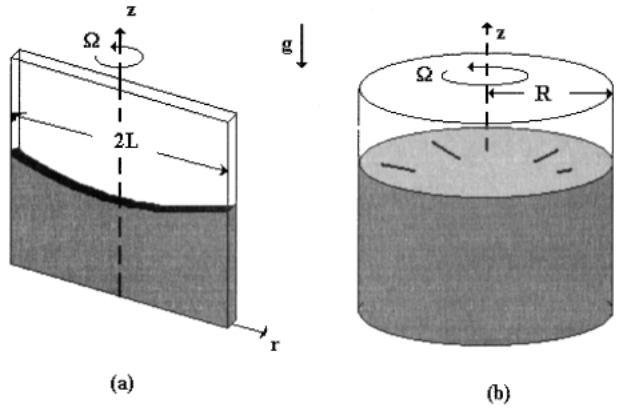

Fig. 3. Schematic view of the free surface deformation of a granular material within (a) a thin rectangular bin and (b) a cylinder. In both cases the systems rotate around its symmetry axis with angular velocity Ω and under the gravity acceleration g.

3.2 *Free surface deformation of sand in a bin under vertical rotation*

The complete history of the free surface deformation of a non cohesive granular media in a thin rectangular bin or a cylinder (Fig. 3), rotating with angular velocity Ω about its axis, can be studied experimentally by using eq. (8) because in this case the surface flow is slow.[24] Using the coordinates r and z for the horizontal and vertical directions [Fig. 3(a)], respectively, we find that the force balance equation of a small element of volume at the free surface of the granular pile, eq. (8), can be written as

$$\rho(\Omega^2 r\cos\theta - g\sin\theta) = \rho(\Omega^2 r\sin\theta + g\cos\theta)\mu\beta. \quad (12)$$

The value of β can be $-1 \le \beta \le 1$, depending on the direction of the friction force, the Froude number (a function of the angular velocity Ω), and the history of how this value is reach together with the initial conditions.

Rearranging terms, scaling the coordinates (z and r) with the length L of the rectangular container and introducing the Froude number $F_r = \Omega^2 L/g$, eq. (12) transforms to the following dimensionless form

$$\tan\theta = \frac{\mathrm{d}z}{\mathrm{d}r} = \frac{F_r r - \mu\beta}{1 + \mu\beta F_r r}. \quad (13)$$

Assuming we slowly increase the Froude number from zero, there is a critical value of the Froude number, $F_r^+ = \mu$, below which the surface does not show any deformation; the superscript plus sign in the Froude number indicates that the state of motion results from increasing F_r, while a superscript minus sign that the state of motion results from decreasing F_r. The solution of eq. (13) for increasing Froude number, is

$$z(r) - z_c = \frac{1}{\mu}(r - r_c) - \frac{1+\mu^2}{\mu^2 F_r}\ln\left(\frac{1+\mu F_r r}{1+\mu F_r r_c}\right), \quad (14)$$

where $1 \ge r \ge r_c$ and corresponds to a critical region with a value of $\beta = 1$. Equation (14) gives the resulting logarithmic surface profile for the critical region.

In the case of decreasing Froude number, we can obtain from eq. (13) with $\beta = -1$, the solution

$$z(r) - z_c = \frac{1}{\mu}(r_c - r) - \frac{1+\mu^2}{\mu^2 F_r^-}\ln\left(\frac{1-\mu F_r^- r}{1-\mu F_r^- r_c}\right), \quad (15)$$

where $0 \le r \le r_c$ is now the critical region. Equation (15) will contain the dependence on the maximum Froude number $F_{r\max}^+$ reached during rotation, in the form

$$F_r^- = \frac{F_{r\max}^+ r_c(1-\mu^2) - 2\mu}{2F_{r\max}^+ r_c^2\mu + r_c(1-\mu^2)}, \quad (16)$$

where z_c can be obtained in both cases using the overall mass conservation. Therefore, for the same value of the Froude number we obtain in this case two different surface equations (i.e., same as found experimentally.[24] In general, there will be an infinite number of possibilities, depending on the history of how we arrives to a given Froude number, showing the strong non-linear character of the problem.

From eq. (13) we recover also the newtonian fluid behavior in the case of $\mu = 0$, the solution of which can be given in dimensionless form as[25]

$$z - z_0 = \frac{F_r}{2} r^2. \quad (17)$$

On the basis of the previous analysis, we can show some shapes of the surface piles resulting from rotation. Assuming we start the motion from rest with an initial flat horizontal surface, we obtain a peak at the center with decreasing height as the Froude number increases. Figure 4 shows two-dimensional projections of the surfaces generated by slowly increasing F_r^+. The lines show the theoretical results while the symbols represent experimental data. Experiments were made using thin rectangular bins with the following dimensions: 30 cm length ($L = 15$ cm), 0.4 cm width and 30 cm height, the bins were filled with Ottawa sand ($\mu = \tan\phi_c = \tan 28^\circ = 0.53$) up to $H = 14$ cm and the Froude number was varied from 0 up to 52.78. We also assumed a value of $\mu = 0.53$ in order to compare the theory with experiments. The values of the chosen Froude number were: $F_r^+ = 4.0$, where a clear central peak is noted, $F_r^+ = 26.14$ and $F_r^+ = 42.57$.

On the other hand, if we decrease the Froude number from $F_{r\max}^+ = 52.78$, we obtain another type of solutions for $F_r^- = 26.14$, $F_r^- = 4.0$ and finally $F_r^- = 0$, where we obtain the final state for the surface as a line with constant slope μ ($\phi_c = 28^\circ$) (see Fig. 5). In all cases presented here, there is a good agreement between theory and experiment, which confirms that the present model describes correctly the phenomenology of the experiment. The experimental values of the surface profiles are found to be slightly below the

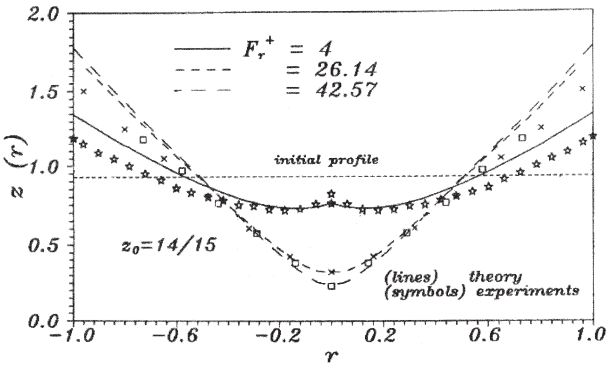

Fig. 4. Free surface profiles obtained from the analysis (lines) and from experiments (symbols) as the Froude number increases, for $F_r^+ = 4$, 26.14 and 42.57.

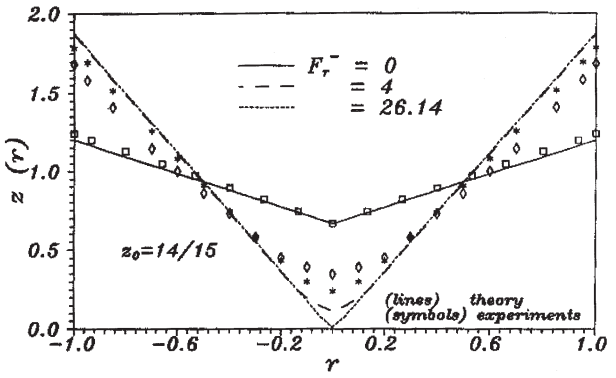

Fig. 5. Free surface profiles obtained from the analysis (lines) and from experiments (symbols) as the Froude number increases, for $F_r^- = 0$, 4 and 26.14.

theoretical ones. We think this is due to the compressibility of the granular material not considered in the analysis.

We should comment that the friction angle actually does not have unique value. It fluctuates within a small range, which in our experiments was $\phi_c \pm \delta$, where $\delta \sim 1^\circ$. For each Froude number, the experimental results deviate a few per cent (less than 2%) from the predicted surface shape profiles.

The free surface deformation in three-dimensional systems (spinning bucket of sand) has been studied theoretical and experimentally.[27] Similar expressions to eqs. (12)–(14) and (17) were obtained in this case. A good experimental agreement was also noted. More recently, the theoretical approach named the BCRE (Bouchad, Cates, Ravi and Edwards) model[26] also has been applied to understand the free surface deformation of a granular sample. In this case the system was prepared with initial slope at the angle $\theta \simeq \phi_c$, and their evolution was studied under abrupt changes in the angular velocity, i.e., unsteady motion.[28] However, to our knowledge this model only is useful when the slope is very near to ϕ_c, i.e., only in cases where there are very small deviations respect to the metastable state. Moreover, quantitative comparison with experiments is difficult.

3.3 *Free surface deformation of sand in a box under uniform linear acceleration*

As other example of the surface's deformation of cohesionless granular material we analyze the free surface evolution of a system under uniform linear acceleration. Like above, the slow flow during linear acceleration of dry granular material within a thin box can be studied by using the balance of force equation and the CYC.[29] In Fig. 6 we show the geometry of the system where H is the initial height and a^* is the magnitude of the acceleration of the box respect to the inertial system fixed to the floor. Since the point of view of an observer in the (x, y) system fixed to the box there exit an acceleration a^* in opposite direction which deforms the surface. So the balance of forces equation [eq. (8)] at the free surface is

$$\rho(a^* \cos\theta - g \sin\theta) = \rho(a^* \sin\theta + g \cos\theta)\mu\beta, \qquad (18)$$

where θ corresponds to the angle related to the horizontal of the free surface. Rearranging terms, scaling the coordinates

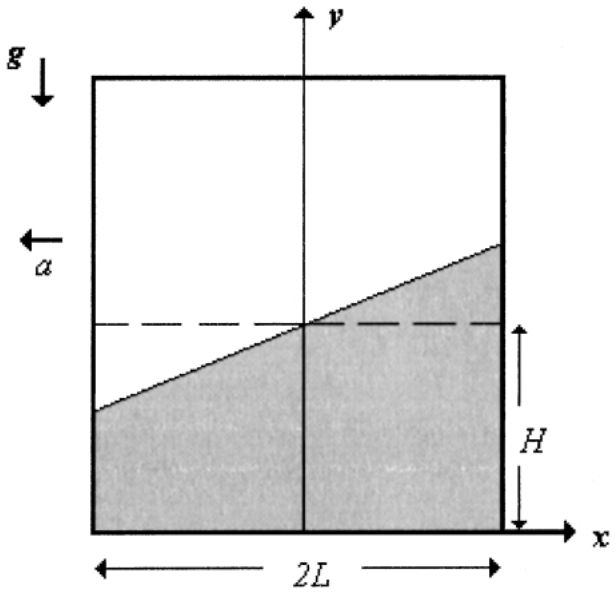

Fig. 6. Schematic view of the free surface of the granular material under horizontal acceleration. The initial height is H, $2L$ is the length of the box and g is the gravity acceleration.

with the half-length, L, of the box and introducing the Froude number $a = a^*/g$, we obtain the dimensionless differential equation

$$\tan\theta = \frac{\mathrm{d}y}{\mathrm{d}x} = \frac{a - \mu\beta}{1 + \mu\beta a}. \qquad (19)$$

We found that there is a critical value of the dimensionless acceleration $a = \mu$ below which the surface does not show any deformation. The solution of eq. (19) for increasing values of the dimensionless acceleration ($\beta = 1$), yields

$$y = \frac{a - \mu}{1 + \mu a} x + \frac{H}{L}, \qquad (20)$$

where we have used the overall mass conservation of granular material. So in a thin box the surface profiles are straight lines with slope $(a - \mu)/(1 + \mu a)$ and at the center always pass with the initial height. Experiments with Ottawa sand ($\mu = 0.53$) let us find a excellent agreement between the theoretical and experimental profiles. Note that like as in a fluid,[25] if $\mu = 0$, the surface profile from eq. (19) is obtained in the form

$$y = ax + \frac{H}{L}. \qquad (21)$$

When the dry granular material is confined in accelerated containers, for example during the transportation of grains, the knowledge of the average forces on the walls of these containers may be useful for example in structural design. This problem was solved analytically in case when there is not a free surface deformation ($a \leq \mu$).[30] The main result in this case was that the forces change as a nonlinear function of the acceleration, a.

4. Fracture in a Dry, Cohesive Granular Medium

The fracture phenomenon has a critical importance in order to optimize some technological applications, such as transport of xerographic powders.[21,31] Moreover, phenomena in cohesive materials under quasistatic deformation

should be treated, in general, at two levels of description: *First*. —The detailed microstructure and the mechanical (surface tension) and electrostatic (Van der Waals) forces of interaction between grains are important and *Second*.— These microscopic forces must be included into a balance of force equation through the values of some phenomenological coefficients. The coefficients could be the cohesion and internal friction of the material and the adhesion (between the substrate and the cohesive granular material). In order to understand the physics of the fracture mechanism in a macroscopic sample of cohesive granular material, we will use this last approach.

In next subsection we present an universal description for the fracture patterns in cohesive granular media under axisymmetrical rotation and gravity action of a sample of cylindrical shape.[20] Comparison with experimental data is also presented in order to validate our approach. So, we nondimensionalize the continuum model presented by Genovese *et al.*,[21] which let us collapse data into a universal curve, when appropriately normalized, simplifying the physical description of this phenomenon. In this way the experimental data, obtained in[21] for a xerographic developer, fit into a single universal curve for both limits of medium and low cohesion

4.1 Universal theory and comparison with experiments

In order to have a direct comparison with experiments where fracture occur, recently has been found experimental evidence of rupture in segments of dry cohesive powders due to tensile load originated during axisymmetrical rotation.[21,31] In these experiments cylindrical cells of xerographic powders, mounted on a horizontal disc, were rotated under the gravity acceleration and fracture patterns such as the one showed in Fig. 7 were obtained. The fracture patterns were characterized through the critical value of the angular velocity, Ω, to produce a fracture in a specimen of radius R, for a series of these xerographic powders having several levels of cohesion. In this work[21] an analysis of this process was made, by using a continuum approach. However, the theoretical analysis for medium and low cohesion can be simplified and generalized by using an asymptotic analysis. In order to do it we will assume, such as in ref. 21, that the fracture occurs for a cylinder of (small) height h with an angle of fracture 2α, bulk density ρ, cohesion coefficient σ_t, internal friction μ and adhesion coefficient (between the substrate and the powder) σ_w. Here, we will assume that the fracture process occurs along a vertical plane as shown in Fig. 7. This is justified because it occurs very frequently in a long series of experiments.[32] However, other fracture shapes should be formed less frequently.[32]

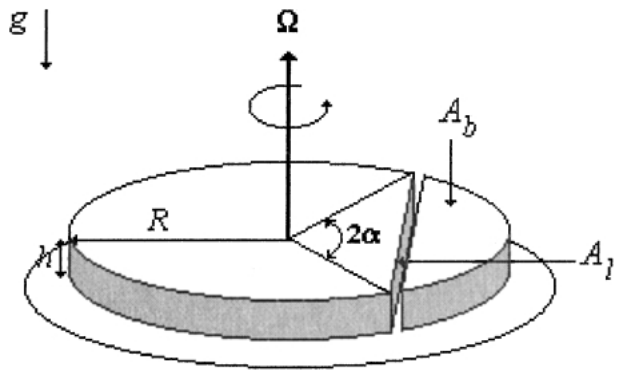

Fig. 7. Schematic illustration of the fracture and the separated slice in a cohesive granular medium under axisymmetrical rotation of magnitude Ω and gravity acceleration g. The slice has a fracture plane of area A_l and the area of this slice in contact with the substrate is denoted by A_b.

The fracture phenomenon was modeled using the CYC. In this last case the CYC gives a relation between the tangential forces along the fracture plane τ, the normal forces to the fracture plane (created during the fracture) N and the cohesive forces C between the segment and the cylinder. In the yield limit, the CYC given by $|\tau| \leq \mu N + C$ produces after a spatial averaging of the forces acting on the segment, the limiting form[21]

$$\rho\Omega^2 RhA_c = \mu\left[\rho g A_b h + \sigma_w A_b\right] + \sigma_t A_l, \tag{22}$$

where A_c is a function represented by

$$A_c(\alpha) = 2R^2\cos^3\alpha\int_0^\alpha \frac{\tan\beta\sin\beta}{\cos^3\beta}\,\mathrm{d}\beta = \frac{2}{3}R^2\sin^3\alpha, \tag{23}$$

The left hand side of eq. (22) corresponds to the centrifugal force on the fractured slice acting in direction normal to the fracture plane. The first term on the right hand side is the adhesion and friction forces, while the second one is due to the cohesion force. A_b and A_l are the contact area of the fractured slice with the substrate and the area of the fracture plane, respectively, and are given by

$$A_b = R^2\left(\alpha - \frac{\sin 2\alpha}{2}\right) \quad \text{and} \quad A_l = 2Rh\sin\alpha. \tag{24}$$

The nondimensional form of eq. (22) can be written as

$$H = Kf(\alpha) + g(\alpha), \tag{25}$$

where

$$H = \frac{\rho g R}{\sigma_t}\mathrm{Fr} \quad \text{with} \quad \mathrm{Fr} = \frac{\Omega^2 R}{g}. \tag{26}$$

In eq. (25) we have assumed that $\alpha \neq 0$. Fr is, as in the previous section, the Froude number and the dimensionless parameter K has the form

$$K = \frac{\rho g R}{\sigma_t}\mu\left(1 + \frac{\sigma_w}{\rho g h}\right) = \frac{\rho g R}{\sigma_t}\mu'. \tag{27}$$

The effective coefficient of friction μ' has the form

$$\mu' = \mu\left(1 + \frac{\sigma_w}{\rho g h}\right). \tag{28}$$

We note easily in eq. (25) that the low cohesion limit $\sigma_t = 0$ is singular i.e., K and H, diverge in this limit. The functions $f(\alpha)$ and $g(\alpha)$ are given by

$$f(\alpha) = \frac{3}{2}\frac{\alpha - \frac{\sin 2\alpha}{2}}{\sin^3\alpha} \quad \text{and} \quad g(\alpha) = \frac{3}{\sin^2\alpha} \tag{29}$$

In the asymptotic limit of high cohesion ($\sigma_t \to \infty$), i.e., $K \ll 1$ ($\alpha \to \pi/2$), it can be easily shown that $f(\alpha) \sim 3\pi/4$, $g(\alpha) \sim 3$, and therefore

$$H \sim \frac{3\pi}{4}K + 3 \quad \text{for} \quad K \to 0. \tag{30}$$

Similarly, in the limit of low cohesion ($\sigma_t \to 0$), i.e., $K \gg$

1 ($\alpha \to 0$), we obtain

$$f(\alpha) \sim 1 + 0.3\alpha^2 + 0.607\alpha^4 \text{ and } g(\alpha) \sim \frac{3}{\alpha^2} + 1 + O(\alpha^2). \tag{31}$$

The value of α which produces the minimum value of H, $\alpha = \alpha^*$, is given in this asymptotic limit

$$\alpha^* \sim \left(\frac{10}{K}\right)^{\frac{1}{4}}, \tag{32}$$

which yields

$$H \sim K + 1.8973\sqrt{K} + 1 + O(K^{-\frac{1}{2}}), \quad \text{for} \quad K \to \infty. \tag{33}$$

The universal behavior $H(K)$ is plotted in Fig. 8 where the continuous line corresponds to this universal curve obtained using a numerical iteration. In order to give a direct comparison between theory and experiments, we have used experimental data corresponding to a granular material referred as a *developer* which is made up of a mixture of toner particles and carrier beads of size around 100 μm. This material plays an essential role in the xerographic process. The data were obtained from experiments reported by Valverde *et al.*[31] and Genovese *et al.*[21] Experiments reported by Genovese *et al.*[21] were made by using developer samples on a substrate (circular disc of 7.52 cm diameter). The cohesive sample has had radius between, $0.2\,\text{cm} \leq R \leq 3.0\,\text{cm}$ and a height of $h = 0.7$ mm. The values for the cohesion coefficient ranged from $\sigma_t = 1.1$ Pa for low cohesion to $\sigma_t = 12.6$ Pa for medium cohesion. The bulk density of the developer was $\rho \sim 3\,\text{gr/cm}^3$. For low cohesion the reported value of μ' was $\mu' \simeq 0.59$, while for medium cohesion $\mu' \simeq 0.62$.[21,31] The Froude number for these experiments varied between $0.54 \leq \text{Fr} \leq 1.21$. In Fig. 8 we show that the data fit very well the universal curve and shows the usefulness and convenience of the employed normalization. The asymptotic limits of high and low cohesion, obtained respectively from eqs. (30) and (33), are plotted as a visual guide. Experiments with very high cohesion were not reported in this case.[21]

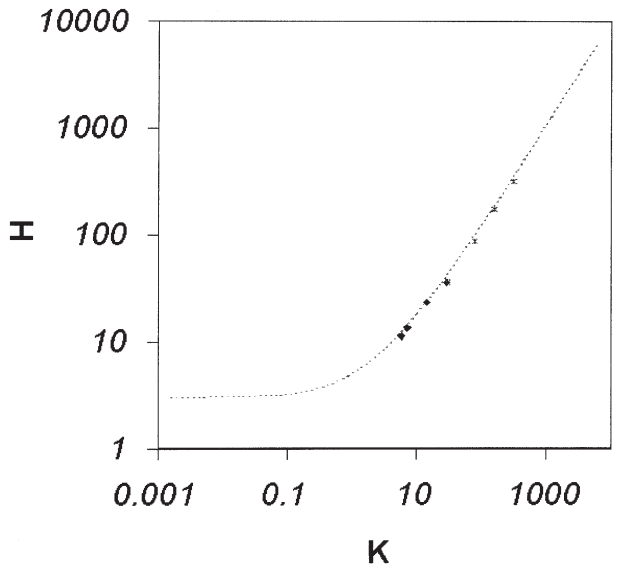

Fig. 8. Log–log plot of H as a function of K for a wide range of values of cohesion. The symbols correspond to experimental data (ref. 21), while the continuous line corresponds to the universal curve obtained using a numerical iteration. Dashed lines indicate the asymptotic solutions for low and high cohesion.

5. Remarks and Conclusions

In this paper we have shown that the continuum treatment, by using the CYC, let us use analytical approaches and, consequently, gives an adequate description for the flow, the free surface deformation and the fracture in granular media in good accordance with the experimental observations. For example, during the horizontal rotation of cohesionless granular material the continuous regime of flow can be easily studied. A power law for the rapid surface current is obtained in accordance with the experiments and independent on the geometry of the container. Due to it our model also gives an adequate basis for the modeling of the dissipative term in the shear stress balance equation during flow.

The problem of the rotation of cohesionless granular material with a vertical axis of rotation, in general is a very complex phenomenon; one must take into account not only the gravitational and the centrifugal forces, but also the history of the motion through the friction force. However, the history or memory effect disappears for continuously increasing or decreasing slow rotation, as the grain achieves the critical state everywhere. In this case, from a continuum point of view, this problem can be understood and a simple analysis can correctly describe the motion. Hysteresis in avalanche processes is related to the changes in the slope near the maximum angle and the frictional and packing factors within the bulk. In this problem the hysteretic behavior is related with these factors but additionally the initial and boundary conditions. Clearly, the accelerated sand box doesn't present this rich phenomenology but the study of this system should be useful, for example, for the structural designers because grain transportation is a very common situation.

Finally, we have deduced an universal description for the fracture patterns in a cohesive granular material. Here the fact the material is dry only was specified in relation to the experimental data (xerographic powders). We showed that the universal curve should actually determine the size and the relative importance of the phenomenological coefficients in this phenomenon. Experiments with materials having very high cohesion were not reported but these materials are not scarce, for instance, $\sigma_t \simeq 50$ kPa for stiff clays (wet cohesive material).[19] So, the obtention of experimental data for a comparison with the theoretical prediction is very important. Work in this direction is in progress.

Acknowledgments

The author acknowledges the valuable discussions with C. Treviño and A. Castellanos. This work has been supported partially by the Mexican Petroleum Institute through the projects FIES 98-58-I and D. 00010 and by CONACyT under the project NC-24.

1) H. Jaeger and S. Nagel: Science **255** (1992) 1523.
2) P. Evesque: Contemp. Phys. **33** (1992) 245.

3) P. Sholtz, M. Bretzand and F. Nori: Contemp. Phys. **38** (1997) 329.
4) L. P. Kadanoff: Rev. Mod. Phys. **17** (1999) 435.
5) P. G. de Gennes: Rev. Mod. Phys. **17** (1999) S374.
6) S. B. Santra, S. Schwazer and H. Herrmann: Phys. Rev. E **54** (1996) 5066.
7) O. Zik, D. Levine, S. G. Lipson, S. Shtrikman and J. Stavans: Phys. Rev. Lett. **73** (1994) 644.
8) O. Reynolds: Philos. Mag. **20** (1885) 469.
9) G. Y. Onoda and E. G. Liniger: Phys. Rev. Lett. **64** (1990) 2727.
10) K. Wieghardt: Ann. Rev. Fluid. Mech. **7** (1975) 89.
11) R. A. Bagnold: Proc. R. Soc. (London) Ser. A **225** (1954) 49.
12) R. A. Bagnold: Proc. R. Soc. (London) Ser. A **295** (1966) 219.
13) S. B. Savage: *Theoretical and Applied Mechanics*, ed. P. Germain and D. Caillere (Elsevier, Amsterdam, 1989) p. 241.
14) S. R. Nagel: Rev. Mod. Phys. **64** (1992) 321.
15) C.-A. Coulomb: *Memoires de Mathématiques et de Physique Présentés á l'Académie Royale des Sciences par divers Savants et Lus dans les Assémbles* (L'imprimiere Royale, Paris, 1773) p. 343 [in French].
16) A. Schofield and P. Wroth: *Critical State of Soil Mechanics* (McGraw-Hill, London, 1968).
17) V. V. Sokolovskii: *Statics of Granular Media* (Pergamon Press, London, 1965).
18) R. L. Brown and J. C. Richards: *Principles of Powders Mechanics* (Pergamon Press, Oxford, 1970).
19) R. M. Nedderman: *Statics and Kinematics of Granular Materials* (Cambridge University Press, London, 1992).
20) A. Medina and C. Treviño: Europhys. Lett. **45** (1999) 269.
21) F. C. Genovese, P. K. Watson, A. Castellanos and A. Ramos: *Powders and Grains 97*, ed. R. P. Behringer and J. T. Jenkins (A. A. Balkema, Rotterdam, 1997) p. 151.
22) G. H. Ristow, F.-X. Riguidel and D. Bideau: J. Phys. I (France) **4** (1994) 1161.
23) J. Rajchenbach: Phys. Rev. Lett. **65** (1990) 2221.
24) A. Medina, E. Luna, R. Alvarado and C. Treviño: Phys. Rev. E **51** (1995) 4621.
25) F. M. White: *Fluid Mechanics* (McGraw Hill, New York, 1994).
26) M. E. Vavrek and G. W. Baxter: Phys. Rev. E **50** (1994) R3353.
27) J.-P. Bouchaud, M. E. Cates, J. Ravi-Prakash and S. Edwards: J. Phys. I (France) **4** (1994) 1383.
28) C. Yeung: Phys. Rev. E **57** (1998) 4528.
29) A. Medina and C. Treviño: Rev. Mex. Fis. **42** (1996) 193.
30) A. Medina and C. Treviño: Rev. Mex. Fis. **44** (1998) 155.
31) J. M. Valverde, A. Ramos, A. Castellanos and P. K. Watson: *Powders and Grains 97*, ed. R. P. Behringer and J. T. Jenkins (A. A. Balkema, Rotterdam, 1997), p. 135.
32) A. Castellanos: 1998, Personal communication.